IS-PORTO 2023 PROCEEDINGS

Proceedings of the 8th International Symposium on DEFORMATION CHARACTERISTICS OF GEOMATERIALS Porto, 3rd - 6th September 2023

Micromechanical observation of kinematics of sheared circular discs

Usman Ali[1], *Mamoru* Kikumoto[1#], *Ying* Cui[1], *Matteo* Ciantia[2], and *Marco* Previtali[2]

[1] *Department of Civil Engineering, Yokohama National University, Japan*
[2] *School of Science and Engineering, University of Dundee, Scotland*
[#]*Corresponding author: kikumoto-mamoru-fc@ynu.ac.jp*

ABSTRACT

Particle rolling is an essential microscopic mechanism that governs macroscopic behavior. This study conducts biaxial shearing tests on bi-dispersed circular discs at different confining pressures. A novel 2D image analysis technique is employed to measure the rolling of all the particles. It is observed that most of the particles exhibit significant rolling during shearing. Rollings are normally distributed in clockwise and counterclockwise directions, and the net rolling of the granular assembly is almost zero. Generally, the rolling of a particle is accompanied by its neighboring particle's opposite rolling in a similar magnitude. In some cases, a group of particles is observed to exhibit rolling in the same direction, accompanied by another opposite rolling group in the neighboring regions. Particles inside the shear band tend to show significant rolling. The rolling rate is prominent at the beginning of the shearing and gradually decreases towards the end. Small particles exhibit significantly higher rotations, while larger particles are relatively resistant to rolling. Small particles work as ball bearings between two big particles, reducing the shear strength of the granular materials. The experimental data obtained in this study can be used to perform detailed validation of numerical models to simulate realistic granular behavior such as DEM.

Keywords: Shearing, circular discs, rolling, shear band.

1. Introduction

The microscopic mechanisms at the particle level govern the macroscopic behavior of granular materials (Calvetti *et al*. 1997). An individual particle can move against the neighboring particles through sliding and rotation at contacts (Iwashita and Oda, 1998). The deformation mechanism of granular media is influenced by frictional sliding between particles (Rowe, 1962; Horne, 1965; Oda, 1972). However, Oda *et al*. (1982) studied the evolution of the microstructure of oval-shaped photoelastic granules in biaxial tests and stated that rotation is the dominant microscopic deformation mechanism. Therefore, image-based experimental techniques have been applied to evaluate granular behavior. Digital image correlation (DIC) is widely used to investigate displacement and deformation fields (Chu *et al*. 1985). Surface-DIC is based on 2D images, while volumetric-DIC (or digital volumetric correlation, DVC) is based on 3D images (Rorato *et al*. 2020).

The microscopic behavior of granular materials had been studied usually in a 2D experiment using rod assemblies (Bardet, 1994). Calvetti *et al*. (1997) studied the micromechanics of multi-sized circular rods using special shear apparatus. Out of 750 rods used in the testing, only 300 in the central part of the shear box were marked with a unique identity. Photos taken during the test were used for measuring micromechanical variables. Furthermore, Misra and Jiang (1997) investigated the deformation patterns of around 600-rod particles of three different sizes in a biaxial test to check the particle rotations. Zhai *et al*. (2018) performed biaxial shearing with 970 oval-shaped particles. Results indicated that particle rotations were an essential micromechanical parameter in macroscopic deformations. However, laboratory observation of particle kinematics is still limited and only obtained on small samples of a few hundred particles. Sibille and Froiio (2007) developed a semi-automated numerical photogrammetry technique for measuring microscale kinematics and the fabric of granular media. They applied it to a biaxially sheared assembly of 1300 wooden rods of circular cross-sections with three different sizes. The interpenetration of wooden rods during shearing affected the accuracy of image analysis. Moreover, due to necessary manual support, processing time was significant. Therefore, they just discussed particle rotation during one load increment. Measuring particle rotations in usual laboratory experiments requires three-dimensional (3D) images of the specimen. Such images can be acquired by X-ray scanning (Hall *et al*. 2010; Andò *et al*. 2012). These 3D images can be correlated using the DVC technique to characterize local particle kinematics. However, X-ray CT can only be applied to static experiments due to the time required for scanning and is affected much by stress relaxation or creep behavior. Alternatively, in 2D systems, surface-DIC only requires 2D images that can be taken with a high-quality digital camera.

Granular behavior is usually simulated by the discrete element method (DEM), wherein individual particles can be modeled explicitly (Cundall 1979). Bardet and Proubet (1991) numerically studied the shear band formation in idealized granular media and confirmed that particle rotations affect granular behavior significantly and concentrate inside shear bands. Kuhn (1999) performed DEM simulations of the biaxial test with

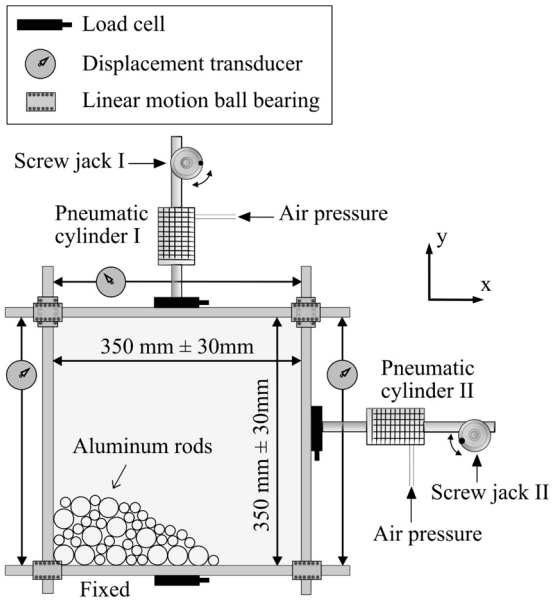

Figure 1. Schematic diagram of biaxial apparatus

circular disks and observed that particle rotations play an essential role in granular deformations. DEM requires acalibration/validation process to confirm the validity of the numerical results. The validation is usually performed by comparing numerical results with the stress-strain response from elementary tests (Nitka *et al*. 2021). Such a validation process may not sufficiently confirm the particle-scale mechanisms in numerical results. In the validation process, consideration of particle scale information is usually overlooked due to insufficient experimental information on idealized circular disks (the usual shape used in DEM).

This study conducts the biaxial shearing test on assemblies of bi-disperse aluminum circular rods using 2674 rods under different confining pressures. A novel 2D image analysis method is used to capture the particles' kinematics. The results confirm that particle rotations contribute significantly to granular deformations. Furthermore, particles exhibiting high rotation are associated with low coordination numbers. This particle scale information can be used to strengthen our understanding of sheared granular media. Additionally, this study provides complete micro and macroscopic information on the shearing of idealized circular disks, which can be utilized for the substantial validation of particle-based simulations such as DEM.

2. Experimental setup

2.1. Biaxial apparatus

Fig. 1 shows a schematic view of the biaxial apparatus. The initial dimensions of the sample box are 350 x 350 mm, and the depth of the walls is 50 mm. The boundaries are rigid walls, wherein the bottom boundary is fixed, and the top and side boundaries move only in the normal direction.

Displacement and load in both axial and lateral directions are measured throughout the test. The axial displacement of the top wall is obtained by averaging the displacements of the right and left ends of the wall. The relative lateral displacement of the side walls is measured

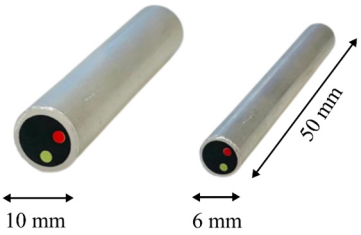

Figure 2. Aluminum rod material used in this study.

by a displacement transducer. Axial and lateral strains are obtained by dividing axial and lateral displacements by the initial height and width, respectively.

The axial load is obtained by averaging the measurements of two load cells installed at the top and bottom walls, and the lateral load was measured by a load cell installed at the right wall. The axial and lateral stresses are calculated by dividing the axial and lateral load by the current changing cross-sectional areas of the specimen perpendicular to the corresponding directions. The load is controlled with the pneumatic cylinder, and the screw jack applies the displacement. The lateral pressure is kept at the same value as the axial pressure to keep the isotropic condition during the consolidation process. During shearing, the lateral pressure is kept constant. For strain-controlled loading during shearing, the axial strain rate is controlled by applying a prescribed displacement by the screw jack. The axial strain rate was selected to ensure the specimen's quasi-static shearing. Further details about the experimental setup can be found in (Ali *et al.* 2023).

2.2. Material used

Aluminum rod material is well known for studying the mechanical behavior of granular materials under plane strain conditions (Schneebeli 1956). Binary mixtures, a mixture of granular materials of two sizes, have attracted attention in the geotechnical field for investigating the mechanical behavior of gravel-soil structures. (Ueda *et al*. 2012). Binary mixtures of aluminum rods mixed in a ratio of 2:3 (big: small) by weight exhibit medium-dense to dense sand behavior (Shahin *et al*. 2004). Fig. 2 shows the granular material used, which consists of dual-size aluminum rods of 10 and 6 mm diameters. The length of the rods is 50 mm, equal to the depth of the biaxial box. Hence, when placed inside the sample box, the material can withstand without any support from the front and back sides and simulates the plane strain condition. The mixing ratio of big to small particles is 2:3 by weight.

2.3. Image analysis

A novel 2D image analysis process extracts particle-level information, such as particle rotations. The bare aluminum has a reflecting silver color which can affect the quality of images taken during the test. To eliminate such issues, the surface of the aluminum rods is treated before testing, wherein black circular stickers are glued on the surface of each particle. A black color sticker on a silver surface helps to acquire high-quality images during the test and facilitates the identification and tracking of

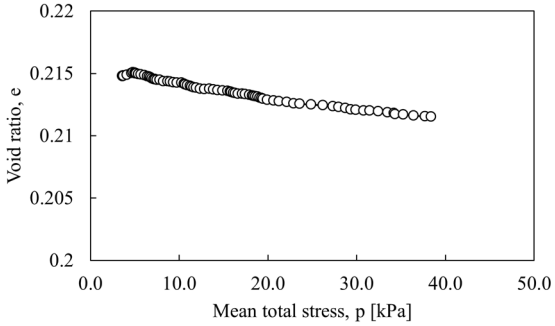

Figure 3. Relationship between void ratio, *e*, and mean stress, *p*, during the isotropic compression

the particles. Additionally, to estimate the rotation of particles, two dots of red and green color are added on a black background to track geometric transformations by digitally correlating two consecutive images taken during the test. During the shearing test, high-quality images of 24.35 megapixels (6016 x 4000) are acquired using a digital camera positioned on the front side of the apparatus. The diameter of circular stickers on big particles corresponds to approximately 80 pixels on a digital image, while that on small particles corresponds to approximately 50 pixels. The images are processed to improve the quality by adjusting the intensity and applying other image adjustment techniques using the freeware ImageJ. A well-known approach, MATLAB's built-in function 'imfindcircles' is used to identify circular particles in images. An algorithm by Crocker and Grier (1996) is employed for tracking particle translations. The trajectories include only the translational movement of the particles, not their rotation. Finally, the algorithm developed by Chen *et al.* (2017) named *Multiscale Analysis for Granular Image Correlation* is used to identify particle rotations. The accuracy of rotation algorithms has been evaluated before application. The average accuracy for particles subjected to the known rotation was more than 97%. The rotation of stickered particles during the biaxial test can be estimated by a correlation between two consecutive images. Further details about the image analysis process can be found in (Ali *et al.* 2023).

3. Results and discussion

3.1. Macroscopic response

Fig. 3 shows the relationship between void ratio, *e*, and mean total stress, *p*, during the isotropic compression process. The initial void ratio for all tests is 0.215. The void ratio decreases gradually with the increase in the mean total stress corresponding to the compression of the sample. Fig. 4 shows aluminum rods' stress-strain relationship and volumetric behavior for the shearing test conducted under a confining pressure (σ_3) of 39.2 kPa. Due to rigid boundaries, the displacement is distributed uniformly within the sample; hence no significant peak in the stress-strain curve is observed. The sample is likely to compress at the start of shearing, and the curve falls below zero axes. Then, the increase of volumetric strain corresponds to dilation. The macroscopic behavior of rods is similar to medium-dense sand.

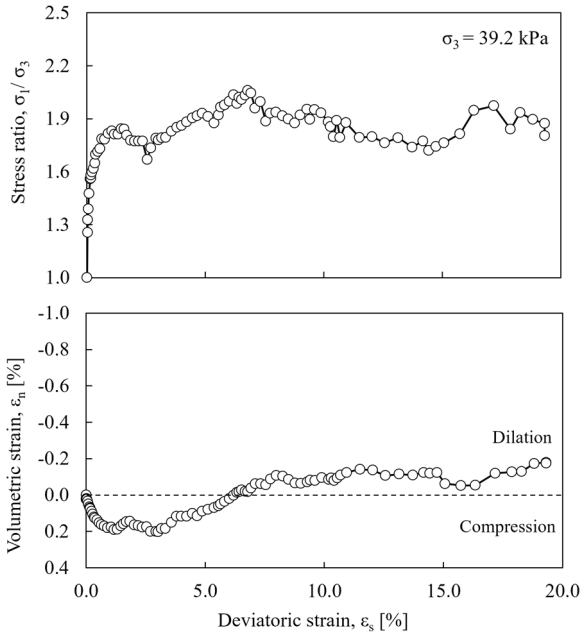

Figure 4. Stress-strain and volumetric behavior of dual-size aluminum rod material

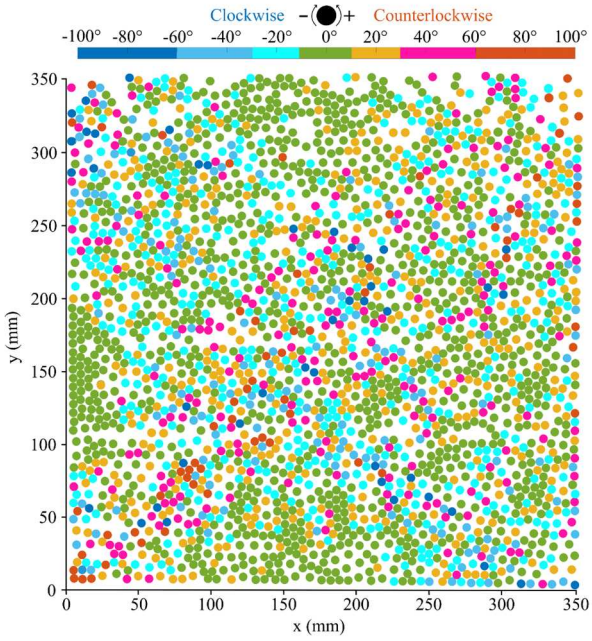

Figure 5. Cumulative particle rotation magnitudes at the end of shearing under σ_3 = 39.2kPa ($\varepsilon_s \approx 20\%$)

3.2. Particle rotations

The rotation of each particle is measured during the shearing process. Out of around 2674 particles used in the test, rotation of more than 2550 particles is identified with a success rate of more than 95 %. Fig. 5 shows the distribution of cumulative rotations at the end of the biaxial shear, deviatoric strain (ε_s) of 20 %, conducted under confining pressure (σ_3) of 39.2kPa. Particles closer to boundaries and along the diagonals of the biaxial box tend to exhibit significant rotations (indicated by blue and red color groups). However, many particles (around 44 % of the total) exhibit minor rotations between -10 to 10 °.

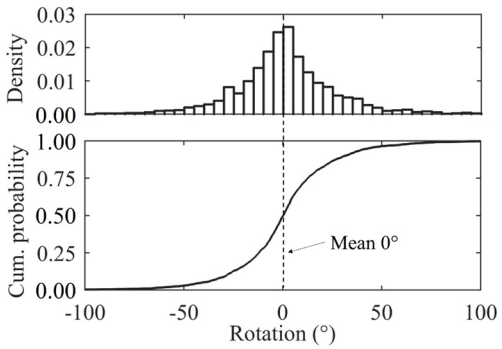

Figure 6. Cumulative distribution of rotation of all particles at the end of shearing under σ_3 = 39.2kPa ($\varepsilon_s \approx 20\%$)

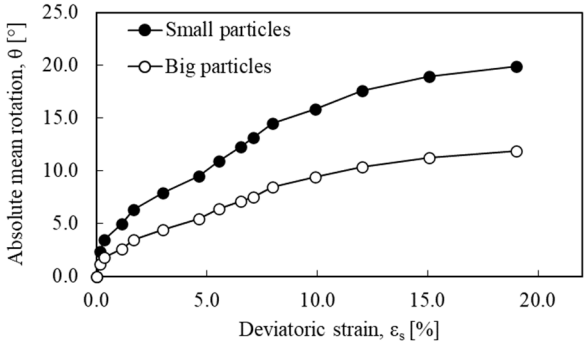

Figure 7. Effect of particle size on the absolute mean cumulative rotation of complete assembly (σ_3 = 39.2kPa)

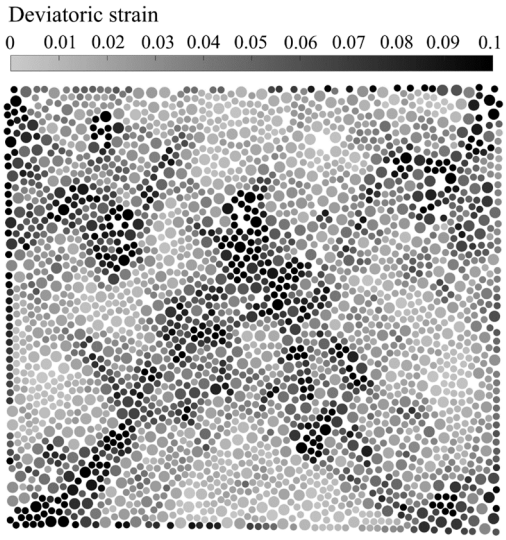

Figure 8. Deviatoric strains of particles during axial strain increment from 8% to 9% for the test under σ_3 = 39.2kPa

Fig. 6 shows the histogram and cumulative distribution of rotation for all particles for the test conducted confining pressure of 39.2 kPa. Generally, the rotation increases with an increase in deformation and mainly falls within 0 ° to ± 50 °. Furthermore, almost half of the particles exhibit clockwise rotations, and the other half exhibit counterclockwise rotations, making the complete assembly's net rotation almost 0 °. The dotted vertical line shows the mean rotation of all particles. Usually, a counterclockwise rotation is accompanied by a clockwise rotation of nearly the same magnitude within the neighboring region. In Fig. 5, red and blue color groups indicate counterclockwise and clockwise rotations, respectively. Mostly blue markers are surrounded by some red or vice versa. In some cases, multiple particles can rotate in the same direction forming a rotation cluster. In such a situation, another opposite rotating cluster of almost the same magnitude can be observed in neighboring regions. The formation of rotation clusters within biaxial assemblies was also observed by Kuhn and Bagi (2002). The mean rotations observed at the end of shearing in clockwise and counterclockwise directions are 18.2° and 19.0°, respectively. Furthermore, the final absolute mean rotation for all the particles in the assembly is 18.6°.

3.3. Particle size effect on rotation

The rotation of small and big particles is analyzed separately to investigate the effect of particle size on rotation magnitude. Of the 2674 particles, 499 are big and 2175 are small. Results indicate that the size of circular particles significantly influences rotational behavior. Small particles undergo high rotation magnitudes; however, big particles are relatively resistant to rotations during granular deformations. Fig. 7 shows the relationship between absolute mean cumulative particle rotation and deviatoric strain for small and big particles. Small particles undergo high rotations as compared to big particles. The absolute mean rotation at the end of shearing for small and big particles is 19.9 ° and 11.9 °, respectively, which indicates that each small particle exhibits around 1.7 times higher rotation magnitude than a big particle on average. Due to the different sizes of particles, the moment of inertia of both sizes is different. The higher mass inertia of big particles relatively obstructs rotations. A similar effect of particle moment of inertia on rotational behavior is observed by Wu *et al*. (2021). Furthermore, the larger circumference of a bigger particles increase the possibility of having multiple contacts resulting in a relatively high coordination number hindering the rotation of big particles. Nie *et al*. (2020) also reported that a higher coordination number obstructs the rotation of particles. Due to high rotations, small particles play the role of ball bearings between big particles, reducing the assembly's overall shear strength. A similar ball-bearing effect induced by the high rotation of small particles is also observed in the DEM simulation of binary granular mixtures by Ueda *et al*. (2012).

3.4. Rotations in shear band

The microstructural constraints on kinematics inside shear bands differ greatly from other parts of the sample during shearing (Rorato *et al*., 2020). Thus, to identify the particles inside the shear band, a nominal deviatoric strain is assigned to each particle using a procedure developed by Catalano *et al*. (2014). This procedure identifies a Voronoi cell for each particle using a regular Delaunay triangulation (Smilauer *et al*., 2015). Thus, the particle positions at two instants towards the end of shearing (i.e., when the axial strain was 8% and 9 %) were identified and introduced in the YADE (*Yet Another Dynamic Engine*). Displacements of neighboring grains were then used to compute a nominal displacement gradient tensor for the triangles whose vertices are the centers of black stickers pasted on each particle. Finally,

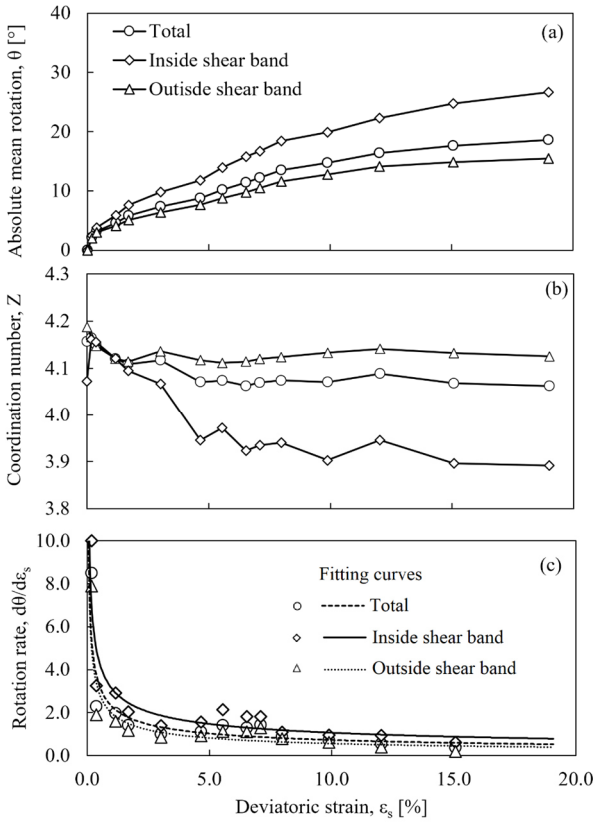

Figure 9. Particle rotations and coordination number evolution inside the shear band (σ_3 = 39.2kPa)

a nominal averaged deviatoric strain was projected back to each grain. Fig. 8 shows the results of the shear band identification process wherein the deviatoric strain can be seen concentrating along the diagonals of the biaxial box, forming two X-shape shear bands. The identified shear bands correspond closely to those apparent high rotation zones in Fig. 5. A threshold value nominal averaged deviatoric strain is set at 0.05 to assign grains to the shear band. Once the particles inside the shear band are identified, the particle levels information, such as rotations and coordination numbers, can be analyzed. Fig. 9a shows the relationship between absolute mean cumulative particle rotation and deviatoric strain for complete assembly, inside and outside the shear band. The absolute mean rotation increases with deviatoric strain. Particles inside the shear band exhibit higher rotations than particles outside the shear band. Outside the shear band, only significant rotations happen at the start of shearing and achieve a steady state towards the end. However, particles inside the shear band continue to rotate even at the end of shearing. This indicates that localized strain inside the shear band is significantly contributed by the rotation of particles along with sliding.

Fig. 9b shows the relationship between the mean coordination number and deviatoric strain for complete assembly, inside and outside the shear band. Generally, the coordination number is higher at the start of shearing and decreases during shearing, corresponding to dilation. Inside the shear band, the coordination number increases at the start, corresponding to the initial compression at the beginning of shearing, then decreasing. The decrease in coordination number is more significant inside the shear band. This indicates that higher rotations inside the

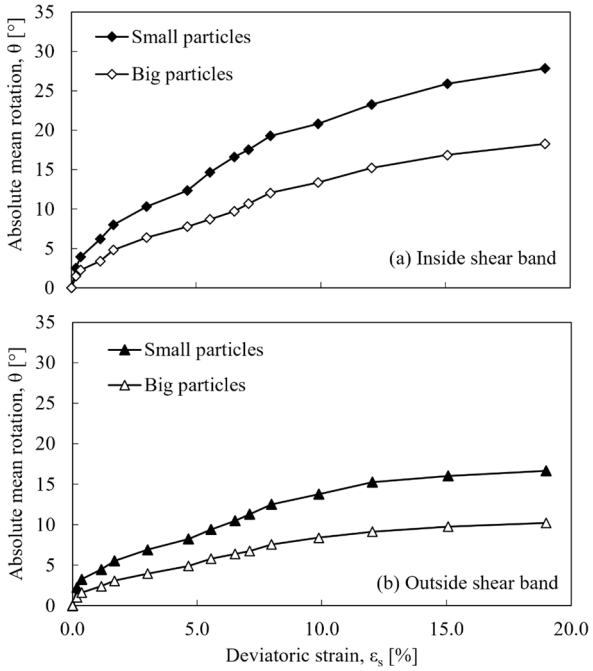

Figure 10. Effect of particle size on absolute mean cumulative rotation (a) inside the shear band (b) outside the shear band (σ_3 = 39.2kPa)

the shear bands are associated with lower coordination numbers. The concentration of particle rotations inside the shear band has also been reported by Bardet (1994), Mitchell and Soga (2005), and Andò *et al*. (2012).

Fig. 9c shows the relationship between rotation rate and deviatoric strain for complete assembly, inside and outside the shear band. Generally, the rotation rate is higher at the start of shearing, corresponding to the initial reorientation of the particles as a reaction to the applied load to find a stable state to resist the applied load. As the shearing progresses, the rotation rate decreases and achieves a relatively steady state towards the end of shearing. The rotation rate inside the shear band is higher, corresponding to the rapid and high rotation of particles inside the shear band.

3.5. Particle size effect in shear band

Particles' rotation is checked to evaluate the effect of particle size inside and outside the shear band based on particle sizes. Fig. 10 shows the absolute mean cumulative particle rotation and deviatoric strain relationship inside and outside the shear band based on the sizes of the particles. It can be seen clearly that either inside or outside the shear band, smaller particles show higher rotation magnitudes. Smaller particles inside the shear band exhibit the most rapid and high rotations, and big particles outside the shear band exhibit the slowest and lesser rotation magnitudes. Significantly higher rotation of small particles inside the shear band will contribute to reducing the shear strength by acting like a ball bearing in between two big particles.

3.6. Confining pressure effect on rotation

Biaxial tests are conducted under three confining pressures σ_3 = 19.6, 39.2, and 58.8 kPa. The rotational behavior is investigated under all three confining

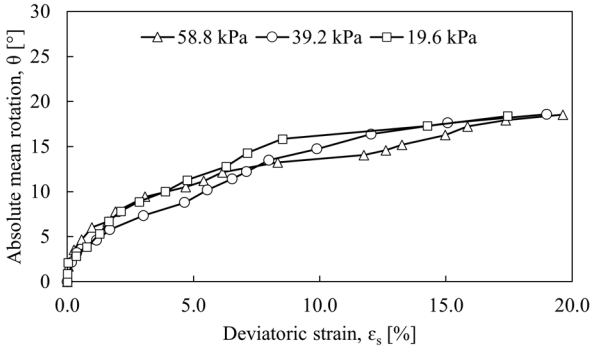

Figure 11. Relationship between absolute mean cumulative rotation and deviatoric strain for different confining pressures

pressures to evaluate the effect of confining pressure. Fig. 11 shows the relationship between the absolute mean cumulative particle rotation and deviatoric strain for three confining pressures. It is observed that the confining pressure has no significant influence on the rotational behavior of particles. The rotational behavior is almost the same regardless of the confining pressure magnitude. The absolute mean rotation for complete assembly at the end of shearing is observed to be 18.56 °, 18.59 °, and 18.54 ° for the confining pressure of 19.6, 39.2, and 58.8 kPa, respectively.

4. Conclusions

Biaxial shearing tests are conducted on dual-size circular assemblies, and the rotation of individual particles is assessed. During shearing, an individual particle interacts with neighboring particles through their contacts and can displace and rotate. The magnitude of displacement and rotation of each particle depends on the particle's location in the assembly and size.

Particles rotate during shearing, and rotation magnitude increases with the increase in axial strain. Most particles exhibit significant rotations during shearing, mainly falling within the range of -50 ° to + 50 °. Around 50.5 % of particles show counterclockwise, 49.5 % indicate clockwise rotations of almost identical magnitudes, and the net rotation of the complete sample is nearly zero. Smaller particles exhibit high rotations and act like ball bearings between big particles, which may reduce the overall shear strengths of assembly. Quick rotations at the start of the test indicate that as the deformation starts, the particles try to stable themselves, and in doing that, they may exhibit quicker rotations. Particles inside the shear band demonstrate higher rotations than particles outside the shear band. Furthermore, the high rotations inside the shear band are associated with low coordination numbers.

Acknowledgments

The Ministry of Education, Culture, Sports, Science, and Technology of Japan is acknowledged for providing financial assistance through the MEXT scholarship to the first author. This work was funded by JSPS KAKENHI under grants 24360192 and 19H00780. Support from the Royal Society IES/R1/201238 International Exchanges grant is also acknowledged.

References

Ali, Usman., Mamoru. Kikumoto, Ying. Cui, Matteo. Ciantia, and Marco. Previtali. 2023. "Role of Particle Rotation in Sheared Granular Media." *Acta Geotechnica* https://doi.org/10.1007/s11440-023-01860-1.

Andò, Edward, Stephen A. Hall, Gioacchino Viggiani, Jacques Desrues, and Pierre Bésuelle. 2012. "Grain-Scale Experimental Investigation of Localised Deformation in Sand: A Discrete Particle Tracking Approach." *Acta Geotechnica* 7 (1): 1–13. https://doi.org/10.1007/s11440-011-0151-6.

Bardet, J. P. 1994. "Observations on the Effects of Particle Rotations on the Failure of Idealized Granular Materials." *Mechanics of Materials* 18 (2): 159–82. https://doi.org/10.1016/0167-6636(94)00006-9.

Bardet, J. P., and J. Proubet. 1991. "A Numerical Investigation of the Structure of Persistent Shear Bands in Granular Media." *Geotechnique* 41 (4): 599–613. https://doi.org/10.1680/geot.1991.41.4.599.

Calvetti, F., G. Combe, and J. Lanier. 1997. "Experimental Micromechanical Analysis of a 2D Granular Material: Relation between Structure Evolution and Loading Path." *Mechanics of Cohesive-Frictional Materials* 2 (2): 121–63. https://doi.org/10.1002/(SICI)1099-1484(199704)2:2<121::AID-CFM27>3.0.CO;2-2.

Catalano, E., B. Chareyre, and E. Barthélémy. 2014. "Pore-Scale Modeling of Fluid-Particles Interaction and Emerging Poromechanical Effects." *International Journal for Numerical and Analytical Methods in Geomechanics* 38 (1): 51–71. https://doi.org/10.1002/nag.2198.

Chen, Zhibo, Mehdi Omidvar, Kaigang Li, and Magued Iskander. 2017. "Particle Rotation of Granular Materials in Plane Strain." *International Journal of Physical Modelling in Geotechnics* 17 (1): 23–40. https://doi.org/10.1680/jphmg.15.00046.

Chu, T. C., W. F. Ranson, and M. A. Sutton. 1985. "Applications of Digital-Image-Correlation Techniques to Experimental Mechanics." *Experimental Mechanics* 25 (3): 232–44. https://doi.org/10.1007/BF02325092.

Crocker, John C., and David G. Grier. 1996. "Methods of Digital Video Microscopy for Colloidal Studies." *Journal of Colloid and Interface Science* 179 (1): 298–310. https://doi.org/10.1006/jcis.1996.0217.

Cundall, P. A. 1979. "A Discrete Numerical Model for Granular Assemblies." *Geeotechnique*. https://www.icevirtuallibrary.com/doi/abs/10.1680/geot.1979.29.1.47.

Hall, S. A., M. Bornert, J. Desrues, Y. Pannier, N. Lenoir, G. Viggiani, and P. Bésuelle. 2010. "Discrete and Continuum Analysis of Localised Deformation in Sand Using X-Ray MCT and Volumetric Digital Image Correlation." *Geotechnique* 60 (5): 315–22. https://doi.org/10.1680/geot.2010.60.5.315.

Horne, M R. 1965. "The Behaviour of an Assembly of Rotund, Rigid, Cohesionless Particles. II." *Proceedings of the Royal Society of London. Series A. Mathematical and Physical Sciences* 286 (1404): 79–97. https://doi.org/10.1098/rspa.1965.0131.

Iwashita, Kazuyoshi, and Masanobu Oda. 1998. "Rolling Resistance At Contacts in Simulation of Shear Band." *Journal of Engineering Mechanics* 124 (March): 285–92.

Kuhn, M R, and K Bagi. 2002. "Particle Rotations in Granular Materials." *15th ASCE Engineering Mechanics Conference* 6 (June 2002).

Kuhn, Matthew R. 1999. "Structured Deformation in Granular Materials." *Mechanics of Materials* 31 (6): 407–29. https://doi.org/10.1016/S0167-6636(99)00010-1.

Misra, A., and H. Jiang. 1997. "Measured Kinematic Fields in the Biaxial Shear of Granular Materials." *Computers and*

Geotechnics 20 (3–4): 267–85. https://doi.org/10.1016/s0266-352x(97)00006-2.

Mitchell, James K., and Kenichi Soga. 2005. *Fundamentals of Soil Behavior*. *Soil Science*. 3rd ed. Vol. 158. New Jersey: John Wiley & Sons, Inc. https://doi.org/10.1097/00010694-199407000-00009.

Nie, Zhihong, Chuanfeng Fang, Jian Gong, and Zhenyu Liang. 2020. "DEM Study on the Effect of Roundness on the Shear Behaviour of Granular Materials." *Computers and Geotechnics* 121 (September 2019): 103457. https://doi.org/10.1016/j.compgeo.2020.103457.

Nitka, M., and A. Grabowski. 2021. "Shear Band Evolution Phenomena in Direct Shear Test Modelled with DEM." *Powder Technology* 391: 369–84. https://doi.org/10.1016/j.powtec.2021.06.025.

Oda, Masanobu. 1972. "The Mechanism of Fabric Changes During Compressional Deformation of Sand." *Soils and Foundations* 12 (2).

Oda, Masanobu, Junichi Konishi, and Siavouche Nemat-Nasser. 1982. "Experimental Micromechanical Evaluation of Strength of Granular Materials: Effects of Particle Rolling." *Mechanics of Materials*, no. 1: 269–83.

Rorato, Riccardo, Marcos Arroyo Alvarez de Toledo, Edward Carlo Giorgio Andò, Antonio Gens, and Gioacchino Viggiani. 2020. "Linking Shape and Rotation of Grains during Triaxial Compression of Sand." *Granular Matter* 22 (4): 1–21. https://doi.org/10.1007/s10035-020-01058-2.

Rowe, P W. 1962. "The Stress-Dilatancy Relation for Static Equilibrium of an Assembly of Particles in Contact." *Proceedings of the Royal Society of London. Series A. Mathematical and Physical Sciences* 269 (1339): 500–527. https://doi.org/10.1098/rspa.1962.0193.

Schneebeli, M. 1956. "Mechanique Des Soils-Une Analogie Mechanique Pour Les Terres sans Cohesion." *Comptes Rendes Hebdomaires Des Seances de l'Academie Des Sciences* 243: 125–26.

Shahin, Hossain M., Teruo Nakai, Masaya Hinokio, Tomoki Kurimoto, and Takashi Sada. 2004. "Influence of Surface Loads and Construction Sequence on Ground Response Due to Tunelling." *Soils and Foundations* 44 (2): 71–84.

Sibille, Luc, and Francesco Froiio. 2007. "A Numerical Photogrammetry Technique for Measuring Microscale Kinematics and Fabric in Schneebeli Materials." *Granular Matter* 9 (3–4): 183–93. https://doi.org/10.1007/s10035-006-0032-0.

Smilauer, Vaclav, Emanuele Catalano, Bruno Chareyre, Sergei Dorofeenko, and Christian Jakob. 2015. "Yade Documentation.", 526. https ://doi.org/10.5281/zenodo.34073.

Ueda, Takao, Takashi Matsushima, and Yasuo Yamada. 2012. "Ball-Bearing Effect on Shear Behavior of Binary Granular Mixture." *Journal of Japan Society of Civil Engineers, Ser. A2 (Applied Mechanics (AM))* 68 (1): 1–9. https://doi.org/10.2208/jscejam.68.1.

Wu, Mengmeng, Linghong Xiong, and Jianfeng Wang. 2021. "DEM Study on Effect of Particle Roundness on Biaxial Shearing of Sand." *Underground Space (China)* 6 (6): 678–94. https://doi.org/10.1016/j.undsp.2021.03.006.

Zhai, L. H., Y. Gao, Q. Yuan, and H. O. Shi. 2018. "Deformation Characterizations of Granular Material in 2D Dense Assembly Subjected to Shearing." *Construction and Building Materials* 158: 1065–72. https://doi.org/10.1016/j.conbuildmat.2017.09.143.